Supporting Information

Dynamic structural transformation induced by defects in nano-rod FeOOH during electrochemical water splitting

*Yitian Hu, Jing zhou, Lili Li, Zhiwei Hu, Taotao Yuan, Chao Jing, Renduo Liu, Shibo Xi, Haiqing Jiang, Jian-Qiang Wang and Linjuan Zhang**

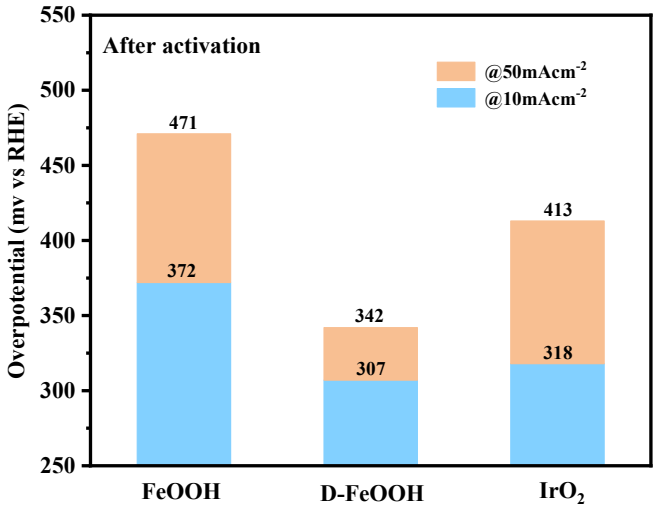

Figure S1. The comparison of overpotential under current density of 10 and 50 mA cm^{-2} for FeOOH and D-FeOOH catalysts after OER activation, along with the benchmark IrO_2 reference.

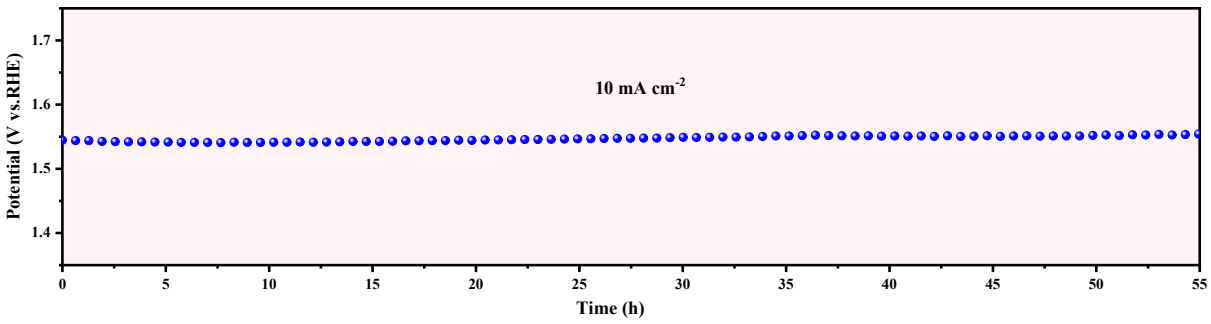

Figure S2. Chronopotentiometric curve of long-term stability for D-FeOOH after activation in 1 M KOH electrolyte at a current density of 10 mA cm^{-2}.

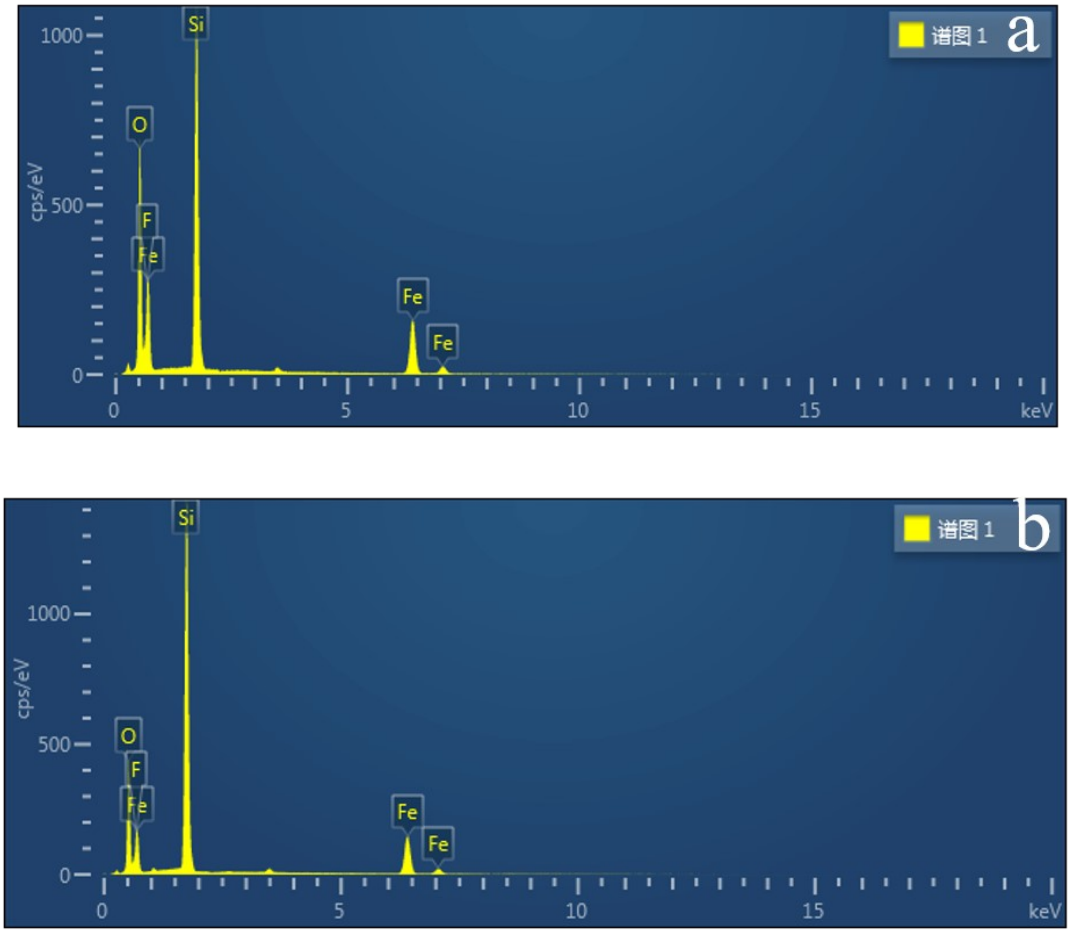

Figure S3. EDS of the as-prepared FeOOH a) and D-FeOOH b).

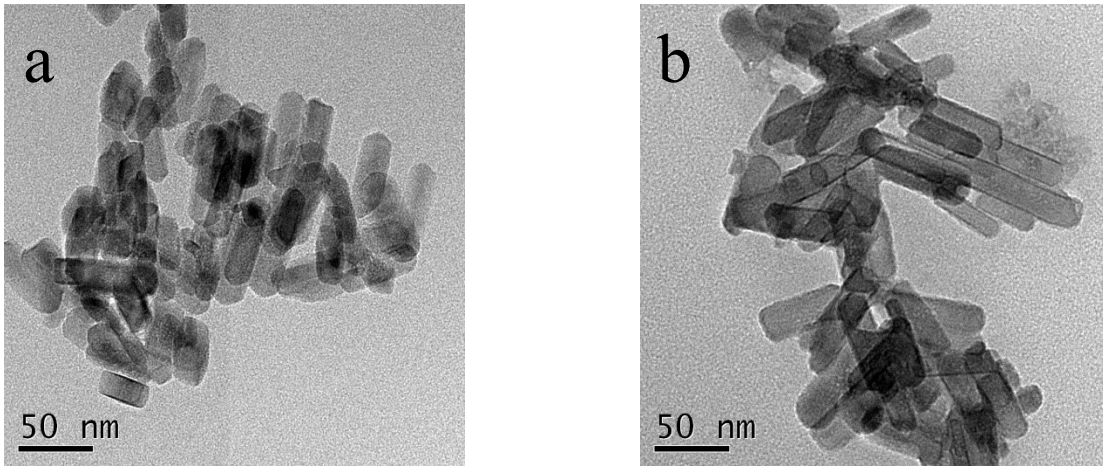

Figure S4. TEM of the FeOOH a) and D-FeOOH b) after OER activation.

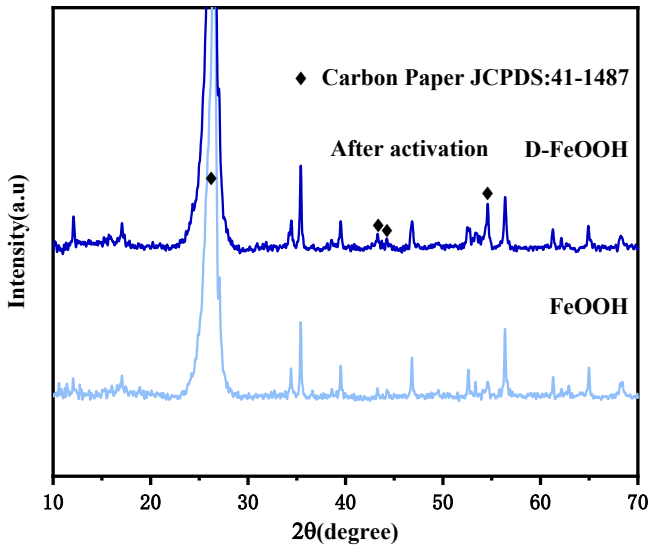

Figure S5. XRD pattern of the FeOOH and D-FeOOH after OER activation.

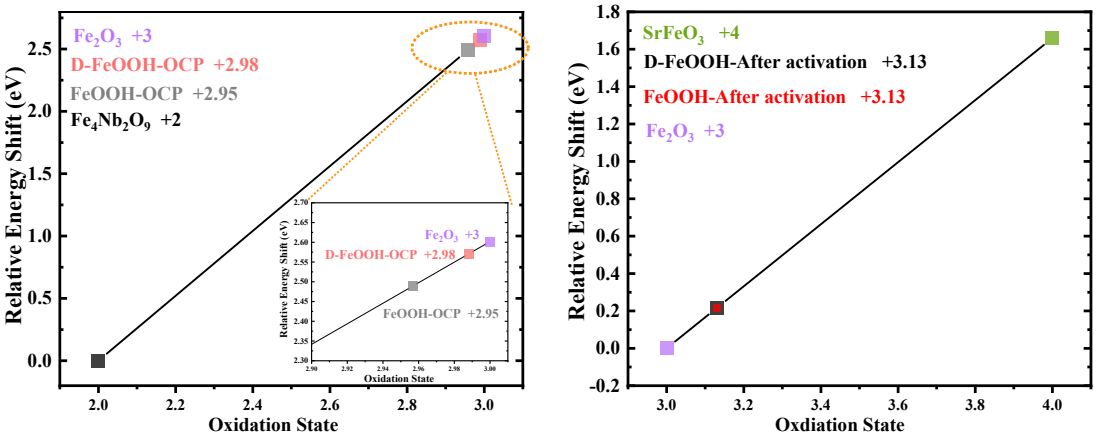

Figure S6 The relative energy positions shift at normalized absorption of 0.8 for Fe K-edge XANES, where $Fe_4Nb_2O_9$, Fe_2O_3 and $SrFeO_3$ were used as pure Fe^{2+}, Fe^{3+} and Fe^{4+} references, respectively.

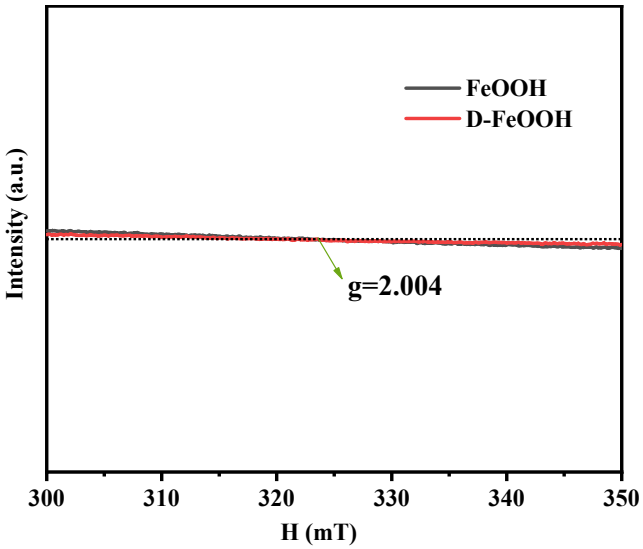

Figure S7 ESR spectra of FeOOH and D-FeOOH.

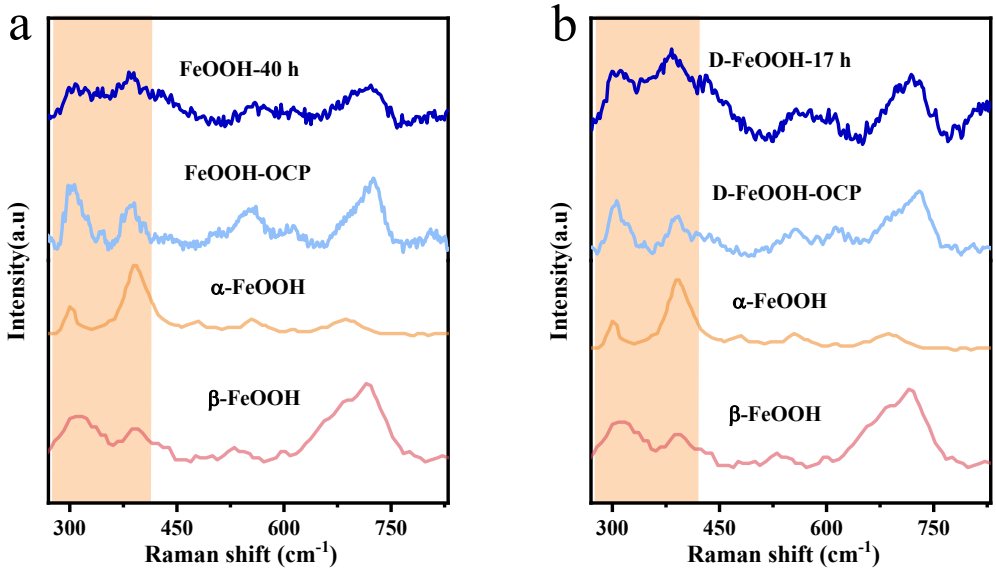

Figure S8. Comparison of Raman spectra for the FeOOH and D-FeOOH samples before and after OER activation, along with the α-FeOOH and β-FeOOH references for comparison as Ref.[1]

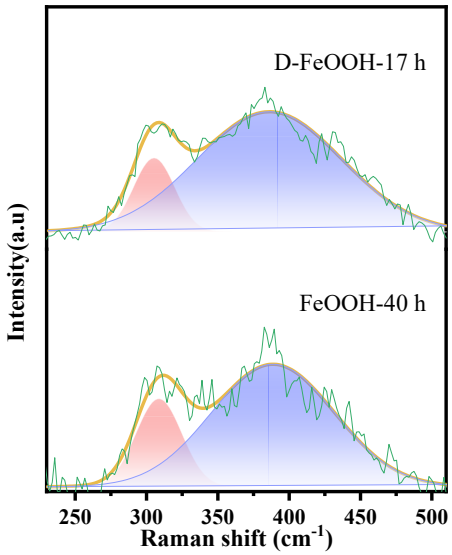

Figure S9. Fit curves of partial in-situ Raman spectra of D-FeOOH-17 h and FeOOH-40 h.

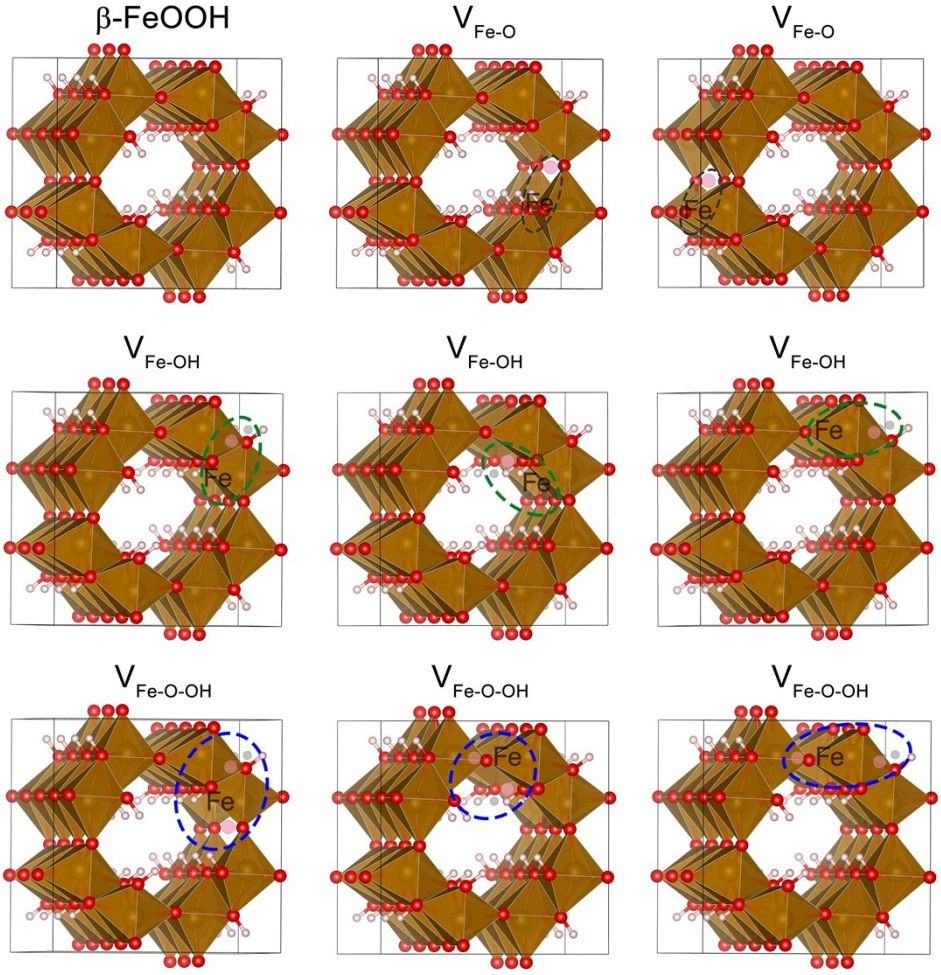

Figure S10. The configurations of β-FeOOH and cluster vacancies in β-FeOOH (defect@β-FeOOH), including V_{Fe-O}, V_{Fe-OH}, and $V_{Fe-O-OH}$. The brown, red, and pink balls represent Fe, O, and H atoms, respectively.

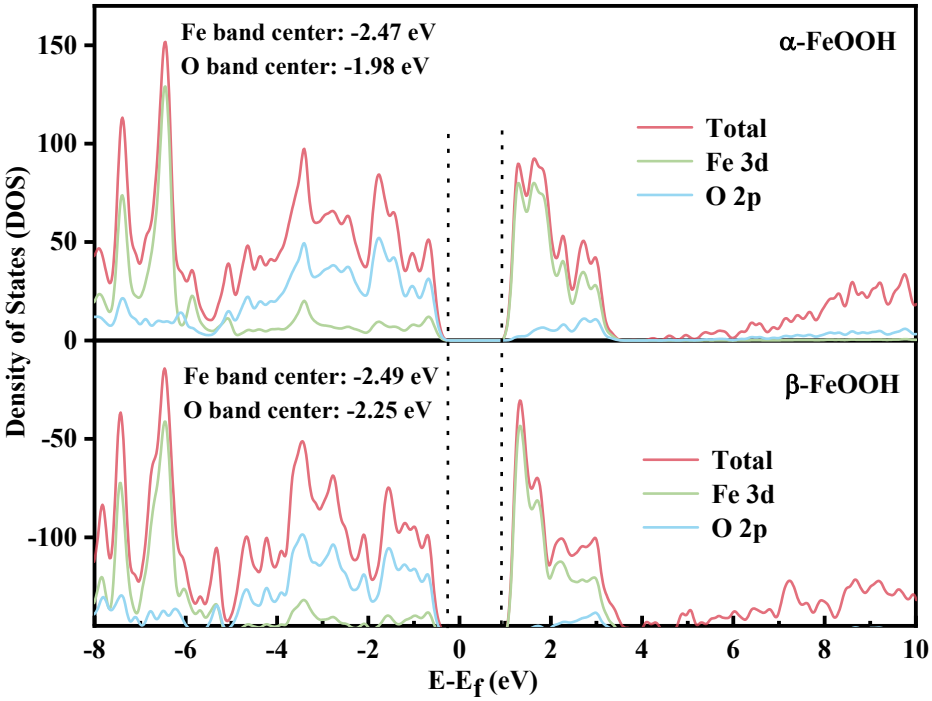

Figure S11. Computed density of states (DOS) of the α-FeOOH and β-FeOOH.

Table S1. The results of High-resolution inductively coupled plasma mass spectroscopy of 3d transition metal elements.

Element / Sample	V	Cr	Mn	Co	Ni	Cu	Zn
FeOOH	0.00011%	0.00790%	0.01108%	0.00087%	0.00293%	0.00174%	0
D-FeOOH	0.00284%	0.00842%	0.00799%	0.00155%	0.00591%	0.00385%	0.00135%

Table S2. Comparison of electrochemical activity for OER of recently reported pure FeOOH

Catalyst	Electrolyte	η（mV） 10 mA cm^{-2}	Tafel slope (mV dec^{-1})	Ref.
D-FeOOH after activation	**1 M KOH**	**307**	**36**	**This work**
FeOOH NSs	1 M KOH	470	107	[2]
FeOOH/CFC	1 M KOH	460	65	[3]
β-like FeOOH	1 M NaOH	490	N.A.	[4]
FeOOH	1 M KOH	480	N.A.	[5]
FeOOH-CC	1 M KOH	440	75.31	[6]
FeOOH powder	1 M KOH	498	131	[7]
FeOOH	1 M KOH	478	107	[8]
β-FeOOH	1 M KOH	400	186	[9]
FeOOH QDs	1 M KOH	490	52.2	[10]
β-FeOOH	1 M KOH	400[a]	163.4	[11]
FeOOH/CFP	1 M KOH	455[a]	131	[12]
FeOOH/CC	1 M KOH	445[a]	N.A.	[13]
FeOOH@CC	1 M KOH	415[a]	49	[14]
FeOOH	1 M KOH	600[a]	57	[14]
FeOOH	1 M KOH	320[a]	N.A.	[15]

[a)]Overpotentials were estimated from the LSV in the reference studies.

Table S3. The lattice parameters for the fully relaxed β-FeOOH and α-FeOOH.

lattice parameters (Å)	β-FeOOH		α-FeOOH		
This work	a=b	c	a	b	c
	10.552	3.072	9.145	10.025	3.043
Ref[16-18]	10.540	3.030	9.028	9.951	3.019
Error	0.11%	1.39%	1.30%	0.74%	0.79%

References

[1] J. Hu, S. Li, J. Chu, S. Niu, J. Wang, Y. Du, Z. Li, X. Han, P. Xu, *ACS Catalysis* **2019**, *9*, 10705-10711.

[2] K. Zhao, X. Ma, S. Lin, Z. Xu, L. Li, *ChemistrySelect* **2020**, *5*, 1890-1895.

[3] X. Yang, B. Xu, S. Zhang, Z. Zhao, Y. Sun, G. Liu, Q. Liu, C. Li, *Int. J. Hydrogen Energy* **2020**, *45*, 9546-9554.

[4] K. Zhu, W. Luo, G. Zhu, J. Wang, Y. Zhu, Z. Zou, W. Huang, *Chem Asian J* **2017**, *12*, 2720-2726.

[5] W. Luo, C. Jiang, Y. Li, S. A. Shevlin, X. Han, K. Qiu, Y. Cheng, Z. Guo, W. Huang, J. Tang, *J. Mater. Chem. A* **2017**, *5*, 2021-2028.

[6] H. Meng, Z. Ren, S. Du, J. Wu, X. Yang, Y. Xue, H. Fu, *Nanoscale* **2018**, *10*, 10971-10978.

[7] P. Ma, S. Luo, Y. Luo, X. Huang, M. Yang, Z. Zhao, F. Yuan, M. Chen, J. Ma, *J Colloid Interface Sci* **2020**, *574*, 241-250.

[8] X. Zhang, B. Zhang, S. Liu, H. Kang, W. Kong, S. Zhang, Y. Shen, B. Yang, *Appl.*

Surf. Sci. **2018**, *436*, 974-980.

[9] Y. Liang, Y. Yu, Y. Huang, Y. Shi, B. Zhang, *J. Mater. Chem. A* **2017**, *5*, 13336-13340.

[10] N. Li, S. Wei, Y. Xu, J. Liu, J. Wu, G. Jia, X. Cui, *Electrochim. Acta* **2018**, *290*, 364-368.

[11] W. Tang, G. Zhang, Y. Qiu, *Int. J. Hydrogen Energy* **2020**, *45*, 28566-28575.

[12] X. Han, C. Yu, J. Yang, X. Song, C. Zhao, S. Li, Y. Zhang, H. Huang, Z. Liu, H. Huang, X. Tan, J. Qiu, *Small* **2019**, *15*, 1901015.

[13] S. Niu, W. J. Jiang, Z. Wei, T. Tang, J. Ma, J. S. Hu, L. J. Wan, *J Am Chem Soc* **2019**, *141*, 7005-7013.

[14] Y. Zhang, G. Jia, H. Wang, B. Ouyang, R. S. Rawat, H. J. Fan, *Mater. Chem. Front.* **2017**, *1*, 709-715.

[15] J. Lee, H. Lee, B. Lim, *J. Ind. Eng. Chem.* **2018**, *58*, 100-104.

[16] X. Han, C. Yu, J. Yang, X. Song, C. Zhao, S. Li, Y. Zhang, H. Huang, Z. Liu, H. Huang, X. Tan, J. Qiu, *Small* **2019**, *15*, 1901015.

[17] E. Zepeda-Alarcon, H. Nakotte, A. F. Gualtieri, G. King, K. Page, S. C. Vogel, H.-W. Wang, H.-R. Wenk, J. Appl. Cryst., 2014, *47*, 1983-1991.

[18] X. Zhang, L. An, J. Yin, P. Xi, Z. Zheng, Y. Du, *Sci. Rep.* **2017**, *7*, 43590.